Quasi-static Testing of a Damage Protected Beam-column Subassembly with Internal Lead Damping Devices

Kevin M Solberg

University of Canterbury, New Zealand

Brendon A Bradley, Geoffrey W Rodgers, John B Mander, Rajesh P Dhakal, J Geoffrey Chase

University of Canterbury, New Zealand

ABSTRACT:

Multiple reversed cyclic quasi-static tests are performed on an 80 percent scale 3D beam column joint subassembly. The physical model is taken from an exterior connection of a jointed precast concrete frame prototype structure that is designed for damage avoidance. Unbonded post-tensioned prestress is provided by high-alloy high-strength threaded bars. Draped and straight tendon profiles are used in the transverse and orthogonal directions, respectively. The joint region is armoured to avoid damage by providing steel plates at the rocking edges of the beam-column interface. Supplemental energy dissipation is provided by high-performance lead-damping devices cast internally in each beam. A combination of couplers and cast in-situ closure pours at the beam ends are used to ensure reasonable construction tolerances. Column axial load and floor dead load are simulated. The global performance of the subassembly and the efficiency of the lead dampers is critically discussed. The subassembly had negligible residual displacements and minimal damage after the test. The hysteresis loops showed stable energy dissipation indicating the success of the dampers. Relatively simple hand methods of predicted performance are shown to conform to the observed experimental behaviour.

1 INTRODUCTION

Research and development of ductile jointed precast concrete structures has gained considerable momentum over the past two decades, with significant research on so-called PRESSS systems being conducted in the United States (Priestley et al., 1999). Jointed precast structures exhibit non-linear response due to connection opening rather than by the formation of a plastic hinge. They have markedly less inherent energy dissipation than ductile monolithic systems. Therefore, supplemental energy dissipation devices are often provided to help reduce displacement response from earthquakes. Various dissipation devices have been investigated (Stanton et al., 1997; Li, 2006; Amaris et al., 2006),but their potential applications are limited by the fact that, for various reasons, they must be replaced following a seismic event. It then becomes apparent that a more robust form of energy dissipation is needed which satisfies the following objectives: (i) the damper should not be at risk of low-cycle fatigue fracture; (ii) the damper should, ideally, be located internally within the beam end region; (iii) residual compression forces in the damper device should creep back towards zero over time; and (iv) the damper device should be economically feasible. In response to these demands, the application of *lead-extrusion* (LE) dampers was developed as part of this study.

While, previous works related to beam-column joints have focused on external dissipation devices, this study will present an attractive alternative whereby LE dampers (Cousins and Porritt, 1993; Rodgers et al., 2006) are buried within the joint, providing a reliable form of energy dissipation and an architecturally pleasing finish. Attention is given to detailing of the joint region to reduce materials and improve constructability while still adhering to the overall objective of ensuring that elements remain damage-free.

2 EXPERIMENTAL INVESTIGATION

2.1 Subassembly Development

An 80 percent scale 3D subassembly was developed, representing an interior joint of a lower floor of a 3x3 ten storey building. The subassembly consisted of two beams cut at their midpoints and an orthogonal beam cut at its midpoint (the approximate location of the point of contraflexure). All beams were 560 mm deep and 400 mm wide and framed into a central 700 mm square column. The orthogonal beam, referred to herein as the gravity beam, was designed for one-way precast flooring panels, while the other two beams, referred to herein as the seismic beams, were designed as part of a seismic moment-resisting frame. These dimensions resulted in a joint moment capacity of 256 kNm (Li, 2006).

Prestress was provided by two 26.5 mm MacAlloy^{TM} threaded bars (f_y = 1100 MPa). The prestressing bars in the seismic direction had a straight profile, whereas the threaded bars in the gravity beam were draped to provide load balancing with the gravity loading from the one-way floor panels. Details of the longitudinal and transverse reinforcement are given in Figure 1, and discussed in detail elsewhere (Solberg, 2007).

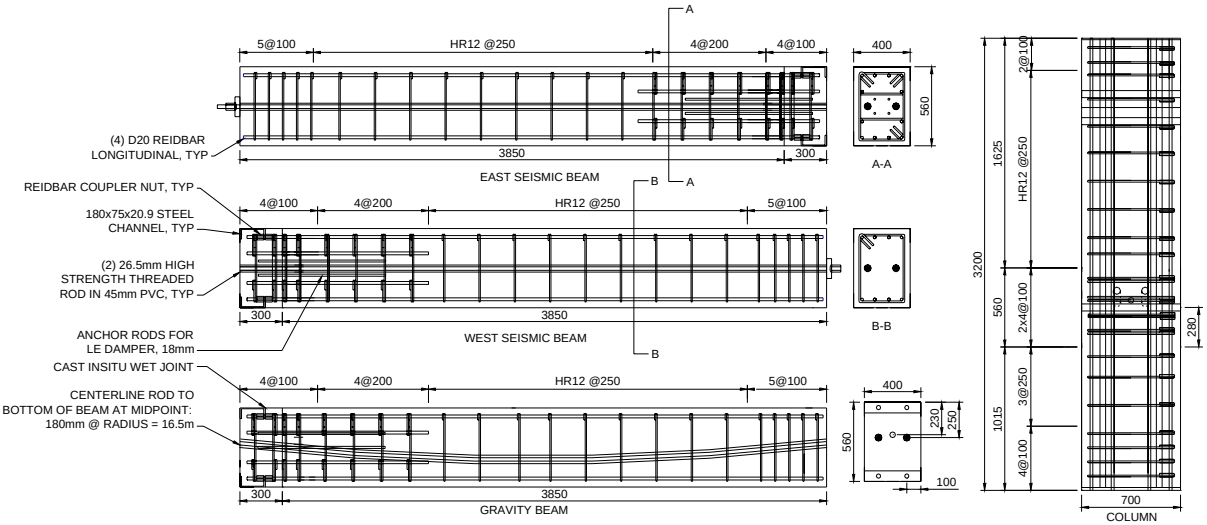

Figure 1: Reinforcement details of the beam-column subassembly elements

A 300 mm cast insitu 'wet' joint was provided at the end of each beam. The detailing strategy of the cast insitu joint in the seismic direction is illustrated in Figure 2a. This joint was designed to accommodate the LE damper with maximum dimensions of 150 mm by 150 mm. This space was provided in the centre of the joint in the seismic beams, and at a 50 mm offset from centreline in the gravity beam. A 180PFC channel was used at the top and bottom to provide the armoured contact surface. The channel also served as a means of mechanically developing the longitudinal reinforcing. This was accomplished by providing cuts on the interior flange of the channel whereby the threaded longitudinal steel could be locked into it using nuts. Furthermore, these nuts provided a means of racheting the channel flush with the column face during on-site fabrication. Four 25x10x500 mm rods were welded in the corners of each flange. These were provided to help stiffen the joint region to ensure rocking behaviour occurred in a rigid manner. Finally, four 1m threaded rods were spaced at 100 mm centres to provide an attachment and anchoring point for the LE damper device.

Shear forces from the gravity and seismic loads were carried by four 30 mm shear keys located at each corner of the connecting beam.

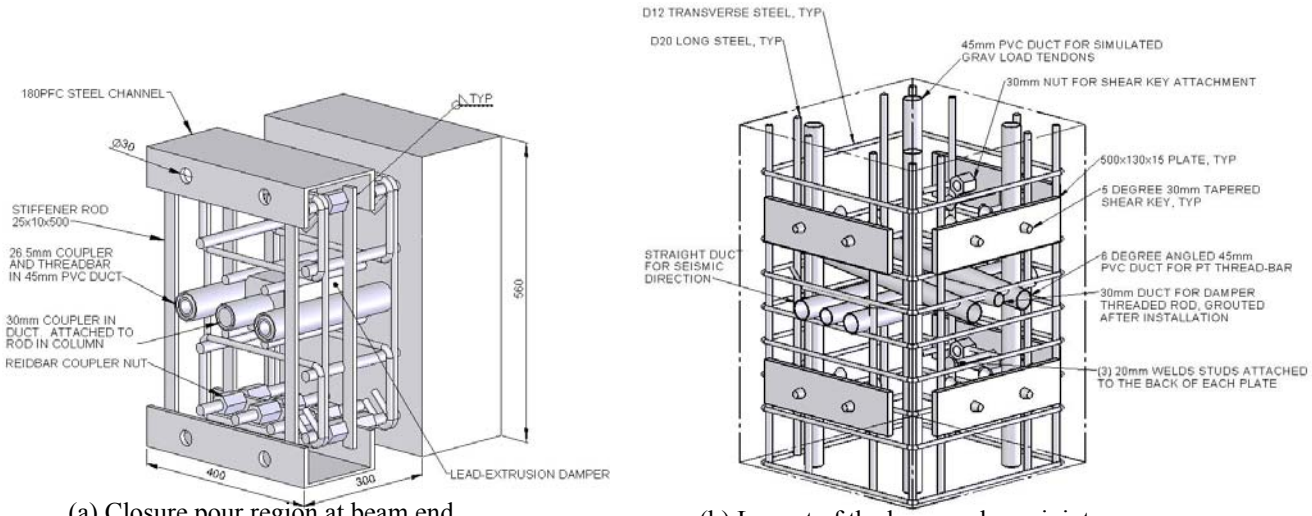

(a) Closure pour region at beam end.

(b) Layout of the beam-column joint.

Figure 2: Geometric layout of the joint detailing

One of the primary objectives of this study was to improve the beam-column joint detailing by improving constructability and reducing materials compared to past designs (Li, 2006). In the column, this was accomplished in several ways, as illustrated in Figure 2b: (i) the column contact plates were reduced from a single full depth plate to two end plates; (ii) the prestress ducts ran straight, rather than angled, in the joint, thus reducing congestion; (iii) the internal dampers in the beam were connected using a single rod with grouting tubes. The column armouring plates were sized to provide a full contact surface for the beam's armouring, and to provide a 10 mm extension on all sides. This plate was then checked to ensure concrete crushing in the column did not occur at the design strength of the connection. The plate was developed into the core of the joint using weld studs. Details of the specimen construction are given elsewhere (Solberg, 2007).

2.2 **The lead-extrusion dampers**

Supplemental damping was provided by LE dampers, as shown in Figure 3a. A single LE damper was designed to fit within in the ends of each beam, as illustrated in Figure 2a. A 30 mm rod with one threaded end was used as the damper shaft (Figure 3a). This rod was designed to be coupled to a threaded rod in the column of the same size. Four 18 mm (f_y = 300 MPa) threaded rods at 100 mm centres were cast into the precast beam and used to anchor the device within the closure pour. The attachment holes on the devices were oversized to allow the device to be adjusted when coupled to the threaded rod in the column.

Given the initial prestress force of 250 kN per threaded bar, the dampers were designed for a 250 kN yield force. This corresponds to a re-centering moment ratio of 1.23 and 1.06 in the NS direction for positive and negative moment, (considering overstrength in the dissipator and reduced prestress force) and 1.13 in the EW direction. Figure 3b presents the force-displacement response of the three damping devices. Devices 1, 2 and 3 were installed in the west, east and south joints of the specimen, respectively. Testing of the LE devices was performed using an Avery^{TM} testing machine. As apparent in the figure, the devices provide similar response.

2.3 **Predicted response**

To arrive at the force-displacement response of the subassembly, first the moment capacity of the joint was assessed. By assuming the members behave in a rigid manner, the moment arm can be taken from the edge of the beam, summing each contribution independently:

$$M = \sum M_{PS} + \sum M_{diss} \tag{1}$$

given that

$$M_{PS}^{\pm} = P_{PS} e_{PS};\ M_{diss}^{\pm} = P_{diss} e_{diss} \tag{2}$$

where e_{PS} = the distance of the from the edge of the beam (280 mm in the EW direction, 310 mm and 250 mm in the NS direction); e_{diss} = the distance of the dissipation device from the edge of the beam (280 mm in the EW direction, 330 mm and 230 mm in the NS direction); P_{PS} = the force in the threaded bars, and P_{diss} = force in the dissipation device. The force in the threaded bars is found by:

$$P_{PS} = P_i + \frac{A_{PS} E_{PS}}{L_t} e_{PS} \theta_{con} n \tag{3}$$

where P_i = initial post-tensioning force (250 kN); E_{PS}= elastic modulus of the threaded bars (170 GPa); A_{PS} = cross sectional area of the threaded bars (552 mm^2); L_t= unbonded length of the threaded bars (9m); θ_{con}= connection rotation; and n = number of joint openings spanned by the threaded bars (taken as 2 in the EW direction and 1 in the NS direction).

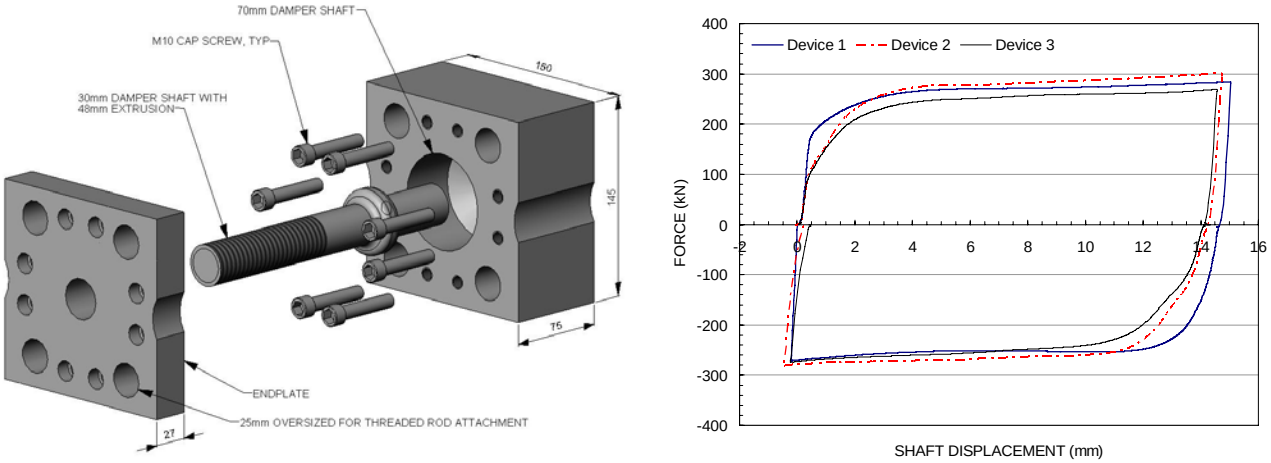

(a) Details of the LE damper (b) Force-displacement response of the damper

Figure 3: Details of the LE damper

The force in the LE dissipation device was found by:

$$P_{diss} = \min \begin{vmatrix} K_{diss} e_{diss} \theta_{con} \\ P_{y,diss} \end{vmatrix} \tag{4}$$

where K_{diss} = stiffness of the dissipation device (200 kN/mm, taken as an average of the three devices) and $P_{y,diss}$ = yield force of the dissipation device (250 kN).

Given the response of the joint, it is possible to identify when the connection begins to open, where the dissipation devices yield, and when the prestress threaded bars yield. In the case of the connection opening, this is assessed by considering the contribution of the initial prestress alone to the moment capacity of the joint. The point at which the dissipation devices yield can be found by setting $P_{diss} = P_{y,diss}$ and solving Equation (4) for θ_{con}. Finally, the onset of yielding of the prestress threaded bars can be calculated from Equation (3) using the yield force of the bars ($P_{PS,yield}$ = 650 kN).

Given a moment-curvature analysis, the force-displacement response of the subassembly can be derived. In the EW direction, the horizontal force at the top of the column, V_{col}, can be correlated to the joint moment by:

$$V_{col} = 2M \frac{L}{L_b L_c} \tag{5}$$

where L = length of the beam to centreline of the column (9.8m); L_b = clear support length of the beam (9.1m); and L_c = storey height (2.8m).

The total top displacement of the system given V_{col} can be attributed to localised rotation at the joint

and the total elastic deformation of the system:

$$\Delta = \Delta_{elastic} + \theta_{con}\frac{L_b}{L}L_c \tag{6}$$

where $\Delta_{elastic}$ is the elastic deformation of the system from flexure. This is defined using the moment area theorem (Solberg, 2007):

$$\Delta_{elastic} = \frac{V_{col,uplift}}{12}\left[\frac{(L_c - D)^3}{EI^*_{col}} + \frac{L_c^{\,2}L_b^{\,3}}{L^2 EI^*_{bm}}\right] \tag{7}$$

where EI^*_{bm} and EI^*_{col} are the effective stiffness of the beam ($0.25EI_{bm,\ gross}$) and column ($0.6EI_{col,\ gross}$), respectively; and D is the depth of the beams (560 mm).

The required moment capacity of the joint (256 kNm) was achieved when the column was at a drift of 1 percent. This was due to the initial prestress force and the full strength of the energy dissipation devices. The localised rotation at the joint at onset of yielding of the prestress threaded bars was found to be 0.052 in the EW direction and 0.053 and 0.043 in the positive and negative NS direction, respectively. This corresponded to a column drift of 6.4 percent in the EW direction and 6.5 and 5.6 percent in the NS direction. Comparisons of the predicted response with experimental results are presented in Section 4.

3 EXPERIMENTAL SETUP

A photograph of the specimen and the test setup is given in Figure 4a, and a plan view is given in Figure 4b. Displacement of the column was provided by two orthogonal actuators attached at the top of the column, while a third actuator was located at the end of the gravity beam to stabilise the specimen. The column was pinned to the floor using a universal joint, additional pins were provided on the struts of each beam. Rotary potentiometers were installed against the opposite face of each actuator. A hydraulic ram was installed at mid-height of the gravity beam to simulate the presence of precast one-way floor panels. This load was spread over a 1.5m timber block. The load was applied at a constant force of 120kN. The base of the column was pinned with a universal joint, allowing free rotation in both the EW and NS direction.

At one end of each prestress threaded bars anchor, load cells were installed to measure the magnitude of the unbonded prestress throughout testing. Four 32mm high strength threaded bars located along the longitudinal axis of the column were each stressed to 500kN to simulate a total axial load of 2000kN ($0.1f'_cA_g$). Potentiometers were located at various locations around the specimen to record displacements during testing.

(a) View of specimen in laboratory

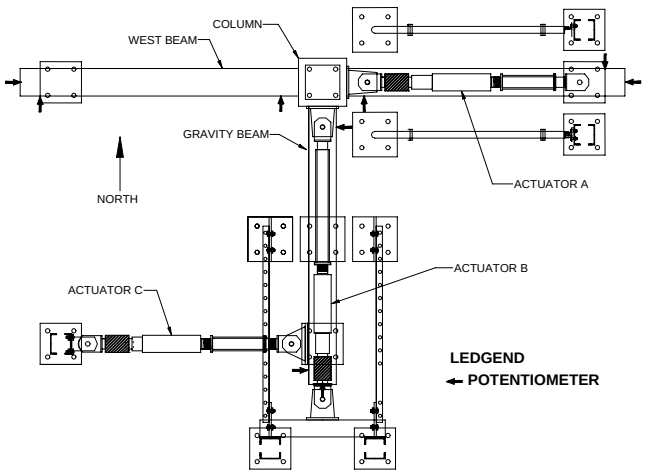

(b) Plan view of the specimen test setup

Figure 4: Isometric view of the specimen test setup

4 EXPERIMENTAL RESULTS

The responses of the subassembly in the EW and NS direction are given in Figure 5. In this quasi-static test, the specimen was subjected to two displacement cycles each at gradually increasing column drifts up to 3 percent. The hand method prediction, using Equations (1)-(7), is plotted on top of the experimental results, showing good agreement. The method predicts the post-gap opening stiffness well. The initial stiffness of the system is slightly higher than observed experimentally. The calculated maximum lateral force at 3 percent drift is within 5 percent of the experimental result. Since the LE dampers exhibited non-linear response, with each damper being slightly different, it was difficult to capture the LE damper contribution; a linear approximation was used with the hand method. Actual test data suggests non-linear response, but the linear approximation seems to fit the experimental data well, though it tends to overestimate strength in the EW direction by about 20 percent. In the NS direction, the prediction was also good. In this case, it was also difficult to predict the contribution from prestress due to its draped profile. This is apparent from Figure 5c which shows the change in prestress force given column displacement. It is obvious that friction between the duct and prestress threaded bars leads to some energy dissipation not considered in the original design. This effect is minor in the EW direction, where the straight ducts reduce the resulting friction.

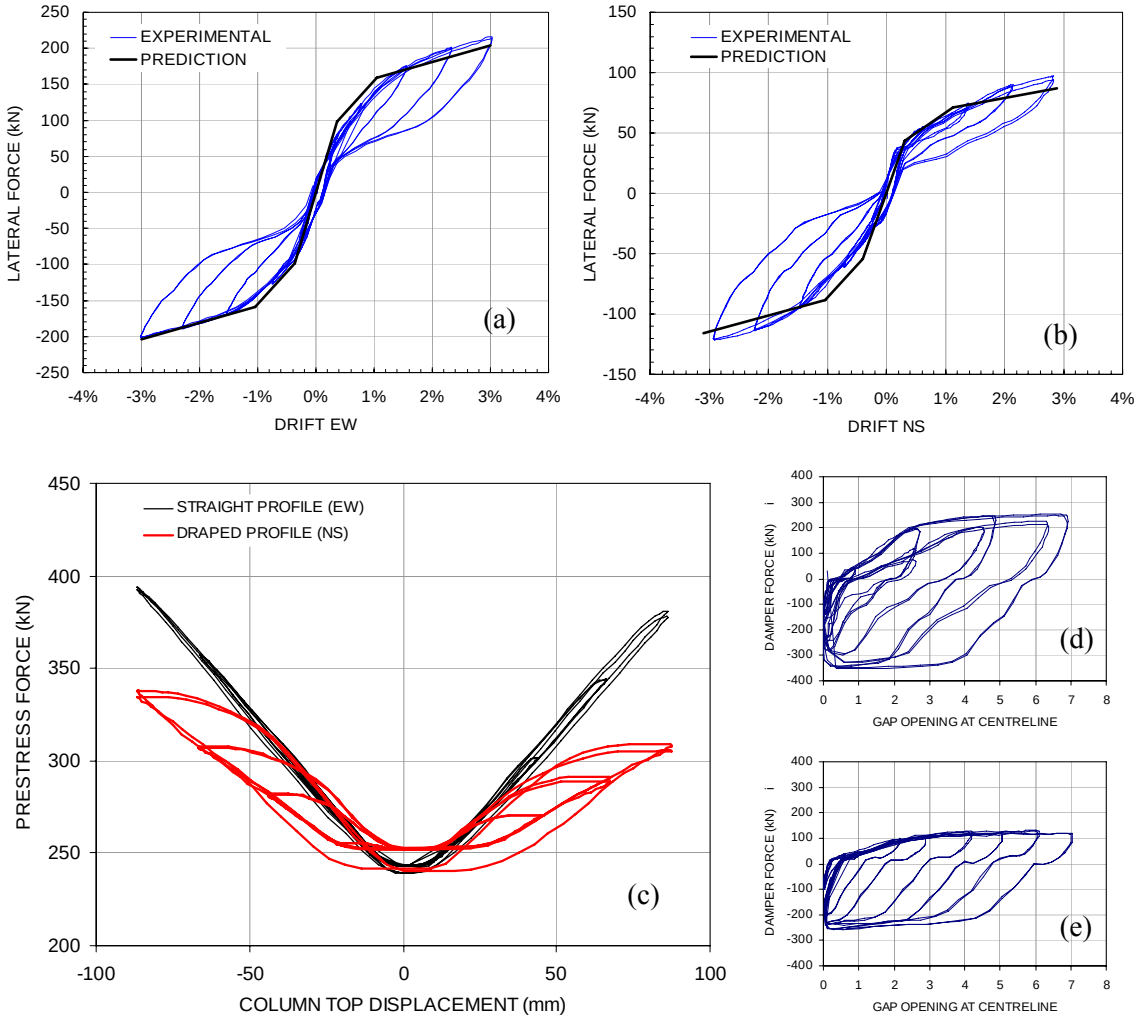

Figure 5: Uni-directional testing to 3 percent drift: Force-displacement response from experimental testing and the hand method prediction: (a) EW direction and (b) NS direction; (c) prestress force; (d) LE damper in gravity beam; and (e) LE damper in east beam.

In the EW direction, excellent hysteretic behaviour is apparent. The specimen does not suffer any noticeable stiffness or strength degradation, and exhibits stable hysteretic energy dissipation. The

maximum recorded residual displacement was approximately 0.08 percent, 1/40th of the maximum drift of 3 percent. The specimen exhibits similar stable energy dissipation in the NS direction also. The maximum residual drift in this direction was recorded to be 0.12 percent, or 4 percent of the maximum drift. This is slightly more than the EW direction, and can be attributed to the aforementioned friction due to the draped tendon profile.

Figure 5d and 5e shows the response of the LE damper in the east seismic beam and gravity beam. It should be noted that due to prestressing, the damper force-gap opening plots are offset by approximately -80 kN. This was recorded using the load cell attached to the coupler and the opening of the joint recorded in line with the devices. The LE dampers performed well, providing significant added energy dissipation every response cycle, in contrast to sacrificial connection and dissipation designs. Problems with load cells were found to the reason for the apparent yielding of the damper in Figure 5e at only 100 kN (instead of 250 kN, which is the case in Figure 5d).

In tension, the stiffness of the LE damper was considerably reduced. This can be attributed to slack within the connecting elements utilized, namely the damper and the threaded rod. This caused the damper to respond to connection-opening after some initial motion. For example, considering only the damper, the device should have reached yield at approximately 0.5 mm of elongation. Instead, yield was not observed until 2.5 mm of elongation. The east damper did not reach its target yield of 250 kN. Instead it initially appears to yield at approximately 100 kN. This may be the reason the initial prediction of response in the EW direction was overestimated. The revised stiffness of the devices, and connecting system considering the connecting elements, was approximately 80 kN/mm and 50 kN/mm for the gravity beam and east seismic beam joint, respectively.

The hand method assumes the moment arm can be taken from the edge of the beam, therefore it assumes rigid-body connection rotation. To validate this, the rotation of the east connection, as measured from three potentiometers across the joint, is given in Figure 6a. The expected (rigid) opening of the joint and the actual behaviour for the joint at 0.025 radians is plotted in Figure 6b. From these plots, it is apparent the rigid body assumption is reasonable. Connection rotation measured from the middle and top potentiometers varies to the order of 10 percent; the difference between the bottom and top potentiometers varies by about 50 percent. Thus, slight rolling of the connection occurred, though this was minimal.

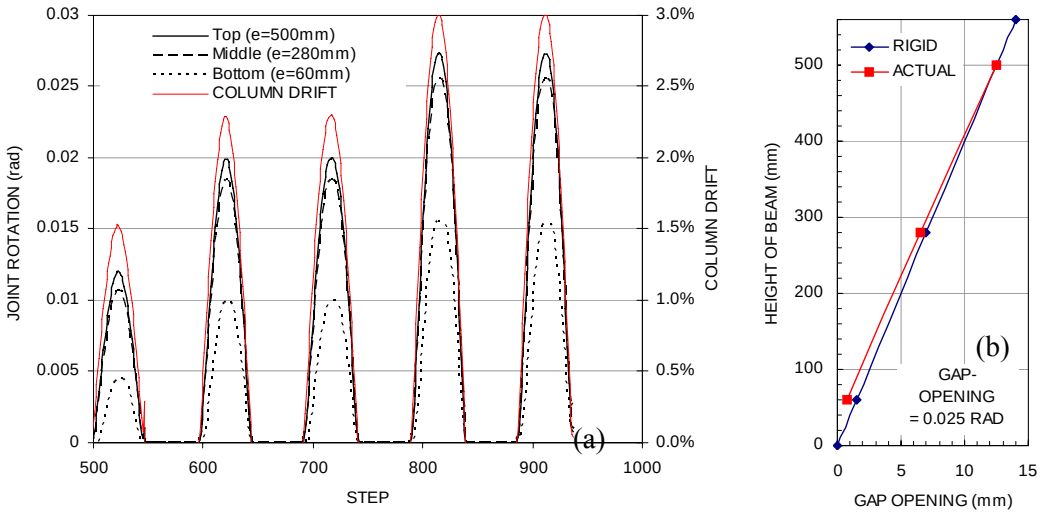

Figure 6: Validation of the rigid-body assumption: (a) joint rotation of east beam measured at three locations along the joint; (b) comparison of rigid versus actual response of the connection. Data is taken from uni-directional QS testing in the EW direction.

Observed damage to the specimen was minimal. During testing, flexural cracks were detected in the beams, spaced at approximately 250 mm spacing. These cracks closed upon unloading. No flexural cracks were observed in the column. Up to 2 percent drift, virtually no cracking was observed in the joint region. Some small cracks, approximately 50 mm in length were observed in the beam's corners

from the end of the channel's flange. These cracks formed when this region was in compression from connection opening. Beyond 2 percent drift, some additional cracks formed, but these were also minor. Again, most cracking was confined to the area around the steel armouring in the beam. No cracks were observed around the armouring in the column, nor were any diagonal shear cracks observed across the joint. No crushing was observed around the column's steel armouring. Upon the completion of testing, there was a prestress loss of about 10 kN per threaded bars in both the EW and NS direction. A photograph of the specimen at a drift of 3 percent is given in Figure 7a and a photograph of the west beam after testing is given in Figure 7b. Note the specimen is essentially damage-free, with all cracks closing upon unloading.

Figure 7: Photographs of the specimen after uni-directional QS testing: (a) the specimen at approximately 3 percent drift; (b) the west beam after completion of testing.

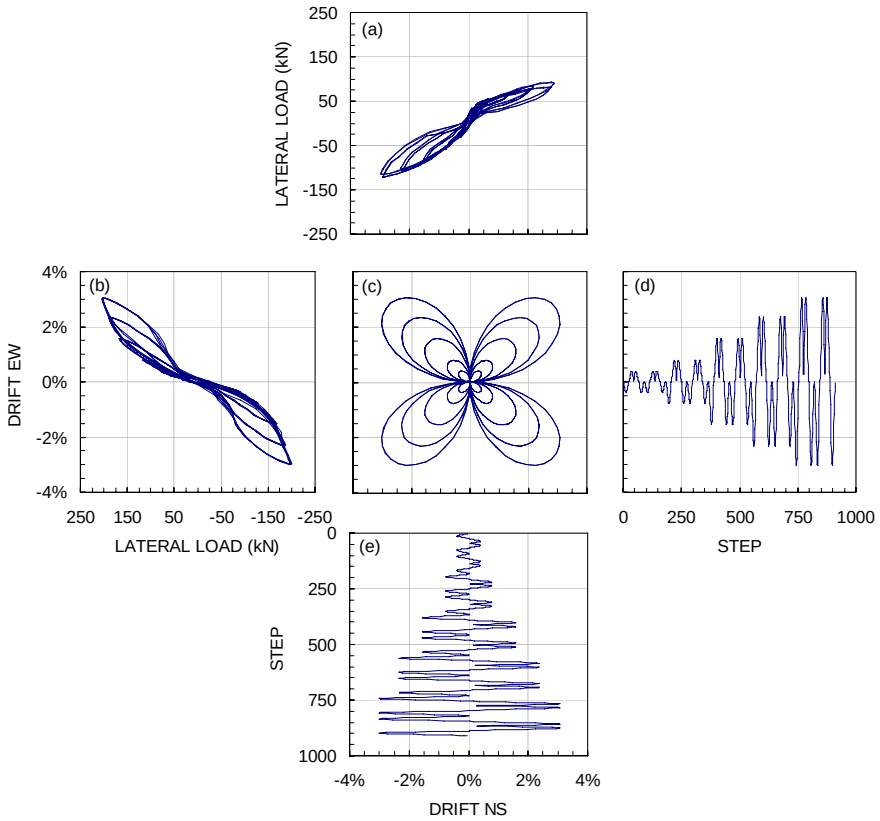

Figure 8: Bi-direction QS testing to 4 percent drift: (a) and (b) give the force-displacement response in the NS and EW direction, respectively; (c) shows a plan view of bi-directional orbit; (d) and (e) give the displacement profiles in the EW and NS directions, respectively.

Results from the bi-directional testing are given in Figure 8, with the bi-directional clover-leaf loading pattern shown in Figure 8c. In this case, the specimen was subjected to two cycles each at 0.5, 1, 2,

and 3 percent drift. As with uni-directional testing, the specimen exhibits a good, stable hysteresis loop. There is negligible stiffness or strength degradation. In the NS direction it is apparent the specimen's unloading cycles are less stable than during uni-directional testing. The bi-directional rocking caused some additional damage to the pier in the form of further crack propagation of cracks from previous tests, on the order of 50-100 mm. These cracks appeared when the specimen was displaced in the EW and NS directions, causing a significant force concentration at the corner of the beams.

5 **CONCLUSIONS**

Based on this investigation the following conclusions can be drawn:

1. An 80 percent scale beam-column joint subassembly was tested under quasi-static loading. The specimen performed well, showing good energy dissipation and reaching drifts of up to 3% with no structural damage requiring repair.
2. A hand method for predicting the response of the system was validated by comparing it to experimental results. The method assumes rigid-body behaviour of the members, allowing the moment arm to be taken from the rocking point. Good agreement between the prediction and experimental results was evident, with discrepancies of about 5 percent.
3. The lead-extrusion damper was able to provide a reliable form of energy dissipation to the specimen.
4. Residual compression forces in the devices at the end of testing were shown to creep back towards zero, with half the force being lost over the first few hours. Therefore, the devices would not have to be replaced following an earthquake.

REFERENCES:

Amaris A, Pampanin S, Palermo A. 2006. Uni and bi-directional quasi-static tests on alternative hybrid precast beam column joint subassemblies. *Proceedings of the 2006 New Zealand Society for Earthquake Engineering* (NZSEE) *Conference*. Napier, New Zealand, Paper #24.

Cousins WJ and Porritt T E. 1993, Improvements to lead-extrusion damper technology. *Bulletin of the New Zealand National Society for Earthquake Engineering*; **26**:342-348.

Li, L. 2006. Further Experiments on Damage Avoidance design of Beam-to-column joints. *ME Thesis*, Dept. of Civil Engineering, University of Canterbury, Christchurch New Zealand

Priestley MJN, Sritharan S, Conley JR, Pampanin S. 1999. Preliminary Results and Conclusions from the PRESSS Five-Storey Precast Concrete Test Building. *PCI Journal*, **44(**6):43-67.

Rodgers GW, Chase JG, Mander JB, Leach NC, Denmead CS. 2007 Experimental Development, Tradeoff Analysis and Design Implementation of High Force-to-Volume Damping Technology. Bulletin of the New Zealand Society of Earthquake Engineering. (in press)

Solberg K.M. 2007. Experimental and financial investigations into the further development of damage avoidance design. *Master of Engineering Thesis.* University of Canterbury, Christchurch, New Zealand.

Stanton JF, Stone WC, and Cheok GS. 1997. A Hybrid Reinforced Precast Frame for Seismic Regions. *PCI Journal*, **42**:20-32.